Interaction of Cardiac Troponin C and Troponin I with W7 in the Presence of Three Functional Regions of Cardiac Troponin I†

Monica X. Li, Ryan M. B. Hoffman, and Brian D. Sykes*

CIHR Group in Protein Structure and Function, Department of Biochemistry, University of Alberta, Edmonton, Alberta, Canada T6G 2H7

Received April 21, 2006; Revised Manuscript Received June 14, 2006

ABSTRACT: W7 is a well-known calmodulin (CaM) antagonist and has been implicated as an inhibitor of the troponin C-mediated Ca^{2+} activation of cardiac muscle contraction. In this study, we use NMR spectroscopy to study binding of W7 to cardiac troponin C (cTnC) free or in complex with cardiac troponin I (cTnI) peptides. Titration of cTnC·$3Ca^{2+}$ with W7 shows that residues throughout the sequence, including the N- and C-domains of cTnC and the central linker, are affected. Analysis of the binding stoichiometry and the trajectories of chemical shift changes indicate that W7 binding occurs at multiple sites. To address the issue of whether multiple-site binding is relevant within the troponin complex, W7 is titrated to a cTnC−cTnI complex (cTnC·$3Ca^{2+}$·$cTnI_{34-71}$·$cTnI_{128-163}$). In the presence of the N-terminal (residues ∼34−71), inhibitory (residues ∼128−147), and switch (residues ∼147−163) regions of cTnI, W7 induces chemical shift changes only in the N-domain and not in the C-domain or the central linker of cTnC. The results indicate that in the presence of cTnI, W7 no longer binds to multiple sites of cTnC but instead binds specifically to the N-domain, and the binding ($K_D = 0.5 \pm 0.1$ mM) can occur together with the switch region of cTnI. Hence, W7 may play a role in directly modulating the Ca^{2+} sensitivity of the regulatory domain of cTnC and the interaction of the switch region of cTnI and cTnC.

As a well-known calmodulin (CaM)[1] antagonist, W7 has been frequently used to explore a wide range of physiological processes that are mediated by Ca^{2+}-CaM. There is considerable evidence that CaM and its antagonists modulate the Ca^{2+} signaling pathway in cardiac myocytes (*1*). The fact that another Ca^{2+}-binding protein, cardiac troponin C (cTnC), exists in abundance in cardiac myocytes has prompted a study of the role of W7 in the interplay of troponin- and myosin-based pathways of Ca^{2+} activation in skeletal and cardiac muscle, which showed that in both skeletal and cardiac muscle fibers, W7 inhibits the maximum ATPase activity and Ca^{2+} sensitivity (*2*). The W7 inhibition is most likely mediated via specific interactions between W7 and TnC. This notion is supported by the observation that W7 binds specifically to TnC and not to tropomyosin, actin, or myosin (*1*).

Like CaM, cTnC is an "elongated" molecule with two globular domains connected by a flexible linker in solution (*3*). Both domains of cTnC contain a core of hydrophobic amino acids, and these residues are essential for binding of cardiac troponin I (cTnI) to cTnC, transmitting the Ca^{2+} signal to other thin filament proteins, signaling the activation of the actomyosin ATPase reaction, and ultimately leading to muscle contraction (for a review, see ref *4*). Structural studies have shown that the apo N-domain of cTnC adopts a "closed" conformation with most of its hydrophobic residues buried (*5*). The energy barrier for "opening" is overcome by the binding of Ca^{2+} and the switch region of cTnI (residues ∼147−163) (*6*, *7*). In the NMR structure of the cNTnC·Ca^{2+}·$cTnI_{147-163}$ complex (*7*) and the X-ray structure of the cTnC·$3Ca^{2+}$·$cTnI_{31-210}$·$cTnT_{183-288}$ complex (*8*), $cTnI_{147-163}$ adopts an α-helical conformation and lies across the hydrophobic groove with contacts to key hydrophobic residues in the N-domain. This interaction initiates the movement of the adjoining inhibitory ($cTnI_{128-147}$) and C-terminal ($cTnI_{163-210}$) regions of cTnI away from the actin−tropomyosin and releases the inhibition. The $cTnI_{34-71}$ region binds tightly to the C-domain of cTnC in the absence or presence of Ca^{2+}. In the X-ray structure of the cTnC·$3Ca^{2+}$·$cTnI_{31-210}$·$cTnT_{183-288}$ complex, the $cTnI_{34-71}$ region forms a long α-helix and makes extensive contacts with the hydrophobic surface of the C-domain of cTnC. Most of the inhibitory region of cTnI is invisible in the core domain structure of the cTnC·$3Ca^{2+}$·$cTnI_{31-210}$·$cTnT_{183-288}$ complex, but the similar region of skeletal TnI (sTnI) is shown to have an extended conformation and interact with the central helix area of skeletal TnC (sTnC) in the X-ray structure of the sTnC·$4Ca^{2+}$·$sTnI_{1-182}$·$sTnT_{156-262}$ complex (*9*). Specifically, the inhibitory region of sTnI was found to make electrostatic contacts with the acidic residues on the central DE helix of sTnC, similar to those observed in the NMR solution structure of the cCTnC·$2Ca^{2+}$·$cTnI_{128-147}$ complex (*10*, *11*).

The hydrophobic patches on both domains of cTnC are essential for binding cTnI and are therefore important targets

† Supported by the Canadian Institutes of Health Research and the Heart and Stroke Foundation of Canada.

* To whom correspondence should be addressed. Phone: (780) 492-5460. Fax: (780) 492-0886. E-mail: brian.sykes@ualberta.ca.

[1] Abbreviations: TnC, troponin C; cTnC, cardiac troponin C; cNTnC, N-domain (residues 1−89) of cTnC; cCTnC, C-domain (residues 91−161) of cTnC; sTnC, skeletal troponin C; CaM, calmodulin; W7, *N*-(6-aminohexyl)-5-chloro-1-naphthalene sulfonamide; J-8, *N*-(8-aminooctyl)-5-iodo-1-naphthalene sulfonamide; TFP, trifluoroperazine.

10.1021/bi060779a CCC: $33.50
Published on Web 07/25/2006

for cardiotonic drugs (usually organic compounds with aromatic groups) used in the therapy of heart conditions (for reviews, see refs *4* and *12*−*15*). Agents such as CaM antagonists TFP and bepridil have been employed for this purpose, and multiple binding sites of TFP and bepridil on cTnC have been identified (*16*). In the X-ray structure of the cTnC·3Ca^{2+}·3bepridil complex, two bepridil molecules pull the N- and C-domains close together to result in a compact structure for cTnC while a third bepridil appears to stabilize an open regulatory domain conformation by binding to the center of the hydrophobic pocket, much like $cTnI_{147-163}$ (*17*). The NMR structure of the cNTnC·Ca^{2+}·$cTnI_{147-163}$·bepridil ternary complex shows that both bepridil and $cTnI_{147-163}$ bind to the hydrophobic pocket of the protein concurrently (*18*). In the structure of cTnC in complex with a Ca^{2+}-sensitizing drug EMD 57033, favorable interactions position EMD 57033 in the hydrophobic pocket of the C-domain with the chiral group making several key contacts with the protein (*19*). In the X-ray structure of the sTnC·4Ca^{2+}·$sTnI_{1-182}$·$sTnT_{156-262}$ complex, a polyoxyethylene detergent molecule, Anapoe, binds specifically to the Ca^{2+}-saturated N-domain of sTnC together with the switch region of sTnI ($sTnI_{115-131}$), and this binding is likely responsible for the increase in the contractile force of muscle fibers in the presence of Anapoe (*9*). Another Ca^{2+}-sensitizing drug, levosimendan, currently used as a treatment for acute heart failure, has been discovered by using cTnC as a target protein, and its Ca^{2+}-sensitizing effect has been shown to be located in the N-domain of cTnC (*14*, *20*).

To elucidate the mechanism of W7 action in cardiac muscle contraction, we have used NMR spectroscopy to study binding of W7 to cTnC free or in complex with cTnI peptides. We use two-dimensional (2D) $^1H-^{15}N$ HSQC and 2D $^1H-^{13}C$ HSQC NMR spectral changes to monitor the titration of cTnC·3Ca^{2+} with W7, the formation of a 1:1:1 cTnC·3Ca^{2+}·$cTnI_{34-71}$·$cTnI_{128-163}$ complex, and the titration of the cTnC·3Ca^{2+}·$cTnI_{34-71}$·$cTnI_{128-163}$ complex with W7. The cTnI peptides that were chosen encompass the three functional regions of cTnI that interact directly with cTnC; as such, the cTnC·3Ca^{2+}·$cTnI_{34-71}$·$cTnI_{128-163}$ complex represents a meaningful cTnC−cTnI model. Our results show that W7 binds to multiple sites of cTnC·3Ca^{2+}, but the binding becomes much simpler in the presence of the cTnI regions; i.e., W7 no longer binds to multiple sites but specifically binds to the N-domain, and this binding can occur together with the switch region of cTnI, $cTnI_{147-163}$. Hence, W7 may play a role in directly modulating the Ca^{2+} sensitivity of the regulatory domain of cTnC and the interaction of the switch region of cTnI and cTnC. These results not only contribute to the understanding of the mechanism of action of W7 in cardiac myocytes but also provide useful information for the design of cardiotonic drugs in general.

EXPERIMENTAL PROCEDURES

Sample Preparation. Recombinant human cTnC (residues 1−161) with the C35S and C84S mutations was used in this study. Since cTnC (C35S/C84S) is the only protein used throughout this work, (C35S/C84S) is omitted in this paper. The engineering of the expression vector and the expression of ^{15}N-labeled and ^{15}N- and ^{13}C-labeled proteins in *Escherichia coli* were as described previously (*21*). Two synthetic cTnI peptides, $cTnI_{34-71}$ (acetyl-AKKKSKISASRKLQLK-TLLLQIAKQELEREAEERGEK-amide) and $cTnI_{128-163}$ (acetyl-TQKIFDLRGKFKRPTLRRVRISADAMMQALL-GARAK-amide), were prepared by the use of standard methodology as described by Tripet et al. (*22*). The sequences were confirmed by amino acid analysis, and the mass was verified by electrospray mass spectrometry. W7 was purchased from Sigma-Aldrich. Two stock solutions of W7 (117.8 and 108.1 mM) in DMSO-d_6 (Cambridge Isotopes Inc.) were prepared, and the vials containing the solutions were wrapped in aluminum foil due to its sensitivity to light. The concentrations were determined by UV absorption using a molar extinction coefficient ($\epsilon_{1cm,297nm}$) of 8060. All NMR samples initially had volumes of 500 μL. The buffer conditions were 100 mM KCl and 10 mM imidazole in a 90% H_2O/10% D_2O mixture, and the pH was 6.7. The NMR samples also contained 0.17 mM DSS, 0.01% NaN_3, and protease inhibitor cocktail I (Calbiochem). Gilson Pipetman P2 and P10 were used to deliver the drug solutions for all titrations.

W7 Titration of cTnC·3Ca^{2+}. To a NMR tube containing a 500 μL sample of 0.81 mM [^{15}N,^{13}C]cTnC·Ca^{2+} were added aliquots of 0.5, 1, 1.5, 2, 3, 4, 4, 4, 4, 6, and 6 μL of 117.8 mM W7 for the 11 titration points. The sample was mixed thoroughly with each addition. The titration was stopped when white precipitate started to appear. The volume increase during titration and the change in protein concentration due to dilution were taken into account for data analysis. The change in pH caused by addition of W7 was negligible. One-dimensional (1D) ^1H, 2D $^1H-^{15}N$ HSQC, and 2D $^1H-^{13}C$ HSQC NMR spectra of cTnC were acquired at every titration point.

W7 Titration of the cTnC·3Ca^{2+}·$cTnI_{34-71}$·$cTnI_{128-163}$ *Complex*. A 1:1:1 [^{15}N]cTnC·$cTnI_{34-71}$·$cTnI_{128-163}$ complex was formed by dissolving solid protein and peptides together in NMR buffer. The protein and peptide concentrations were determined gravimetrically and calibrated on the basis of amino acid analysis of each individual component. The final sample contains 0.48 mM cTnC, 0.48 mM $cTnI_{128-163}$, and 0.48 mM $cTnI_{34-71}$. The pH was adjusted to 6.7, and a slight amount of precipitate was eliminated by filtration. To a NMR tube containing a 500 μL sample of the 1:1:1 complex were added aliquots of 0.5, 1, 1.5, 2, 3, 4, 6, and 10 μL of 108.1 mM W7 for the eight titration points. The sample was mixed thoroughly with each addition. The titration was stopped when white precipitate started to appear (after the 10 μL addition). The volume increase during titration and the change in protein concentration due to dilution were taken into account for data analysis. The change in pH caused by addition of W7 was negligible. 1D ^1H and 2D $^1H-^{15}N$ HSQC NMR spectra of cTnC were acquired at every titration point.

NMR Spectroscopy. All of the NMR spectra were obtained using a Varian INOVA 500 MHz spectrometer at 30 °C. All 1D ^1H, 2D $^1H-^{15}N$ HSQC, and 2D $^1H-^{13}C$ HSQC spectra were acquired using the pulse sequences from BioPack (Varian Inc.). Spectral processing and analyses were accomplished with VNMR (Varian Inc.) and NMRPipe (*23*) and referenced according to the IUPAC conventions.

RESULTS

Binding of W7 to cTnC·3Ca^{2+}. The 2D $^1H-^{15}N$ HSQC NMR spectrum of cTnC·3Ca^{2+} has been assigned (*3*) and

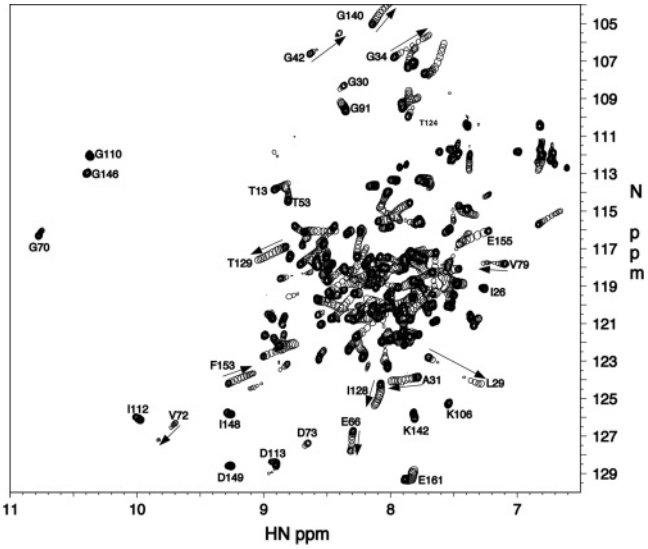

FIGURE 1: Titration of cTnC·3Ca^{2+} with W7. 2D ^{1}H−^{15}N HSQC NMR spectra from the backbone amide regions of cTnC at various W7 additions are superimposed, showing the progressive shift of peaks with increasing $[W7]_{total}/[cTnC]_{total}$ ratios (0.00, 0.16, 0.47, 0.95, 1.58, 2.52, 3.78, 5.04, 6.30, 7.56, and 9.45).

was used as a starting point to monitor W7-induced spectral changes. Figure 1 shows the W7-induced backbone amide resonance shifts in cTnC·3Ca^{2+} as the W7:cTnC·3Ca^{2+} molar ratio increases from 0 to 9.45. Residues throughout cTnC are affected to various degrees. It is interesting to notice that the shifting of the cross-peaks does not stop even when the W7:cTnC·3Ca^{2+} molar ratio reaches 9.45. This observation suggests a relative weak affinity of W7 for cTnC·3Ca^{2+} since cTnC·3Ca^{2+} is not saturated at 7.7 mM W7. It also implies multisite or nonspecific binding of W7 to cTnC·3Ca^{2+}, which is supported by the observation that some cross-peaks shift in a nonlinear fashion (e.g., T124, I128, and E161), as observed in the cases of binding of TFP to cTnC (*16*), binding of W7 to CaM (*24*), binding of W7 to cNTnC and cCTnC (*25*), and binding of J8 to CaM (*26*). The multisite binding mechanism is also reflected in the differences in the cross-peak shift trajectories between the N-domain and the C-domain. Figure 1 shows that most of the C-domain residue peaks gradually shift with little change in their intensity, indicating that the rate of exchange between W7 and the C-domain is fast on the NMR time scale. However, several N-domain resonances, such as L29, G42, and V79, are broadened upon addition of W7, indicating that the binding of W7 to the N-domain occurs with slow or intermediate exchange kinetics on the NMR time scale. For example, the shifts of G42 in the N-domain and T129 in the C-domain are similar in magnitude, yet G42 experiences line broadening during the titration but not T129. This suggests that binding of W7 to the N-domain is tighter, with slower exchange kinetics, than binding to the C-domain. This is consistent with our previous work on binding of W7 to isolated N- and C-domains of cTnC (*25*). Residues in the central linker of cTnC (e.g., G91) also undergo W7-induced chemical shift changes. The binding of W7 to this region may cause the bending of the flexible central linker so the two domains face each other and form a hydrophobic cavity to accommodate several molecules of W7 similar to those observed in cases of cTnC·3Ca^{2+}·3bepridil (*17*), CaM·4Ca^{2+}·TFP (*27*), CaM·4Ca^{2+}·4TFP (*28*), and CaM·4Ca^{2+}·2W7 (*24*) complexes.

The complex stoichiometry of binding of W7 to cTnC·3Ca^{2+} is also demonstrated in Figure 2, which shows the 2D ^{1}H−^{13}C HSQC NMR spectral changes in the methionine methyl region of cTnC with various equivalents of added W7. Like the backbone amides, the methionine methyls undergo continuing spectral changes as the W7:cTnC·3Ca^{2+} molar ratio increases from 0 to 9.45. The methionine methyls are present in the hydrophobic pockets of both the N- and C-domains of cTnC, and many are likely involved in direct contacts with the binding ligands. These groups have been used as site-specific structural markers of cTnC to identify drug binding sites for TFP and bepridil (*16*), EMD 57033, and levosimendan (*29*). In Figure 2, the left-most panel (W7:cTnC·3Ca^{2+} molar ratio of 0) has been assigned on the basis of Sia et al. (*3*), and the right-most panel (W7:cTnC·3Ca^{2+} molar ratio of 9.45) is labeled on the basis of the assignments for cNTnC·Ca^{2+} and cCTnC·2Ca^{2+} in W7-bound states (*25*). Most of the methyl groups exhibit high-field shifts, and these groups are from both the N-domain (e.g., M80 and M81) and the C-domain (e.g., M137 and M157) of cTnC.

*Binding of W7 to the cTn*C·3Ca^{2+}·cTnI$_{34-71}$·cTnI$_{128-163}$ Complex. The formation of a 1:1:1 cTnC·3Ca^{2+}·cTnI$_{34-71}$·cTnI$_{128-163}$ complex was monitored by 2D ^{1}H−^{15}N HSQC NMR spectroscopy as shown in Figure 3A. We assigned the outlying resonances in Figure 3A on the basis of results from previous titrations: cTnI$_{34-71}$ to the isolated C-domain cCTnC·2Ca^{2+} (*19*) and to intact cTnC·3Ca^{2+} (*21*), cTnI$_{128-147}$ to the isolated C-domain cCTnC·2Ca^{2+} (*10*) and to intact cTnC·3Ca^{2+} (*21*), and cTnI$_{147-163}$ to the isolated N-domain cNTnC·Ca^{2+} (*7*) and to intact cTnC·3Ca^{2+} (*21*). These assignments allow us to monitor the titration of the cTnC·3Ca^{2+}·cTnI$_{34-71}$·cTnI$_{128-163}$ complex with W7 (Figure 3B). Among the assigned residues, it is clear that only the N-domain residues (e.g., G34, G42, G49, T53, E66, G68, G70, D73, and V79) but not the C-domain residues (e.g., G110, I112, D113, I128, T129, and F153) undergo chemical shift changes. For a more focused comparison, we show an expanded region of the 2D ^{1}H−^{15}N HSQC NMR spectra covering the three characteristic Ca^{2+}-binding site glycines, G70, G110, and G146 (Figure 3C,D). In Figure 3C, the chemical shift changes of G70 reflect the binding of cTnI$_{147-163}$ to the N-domain of cTnC while those of G110 and G146 reflect the binding of cTnI$_{128-147}$ and/or cTnI$_{34-71}$ to the C-domain of cTnC. When W7 is titrated into the cTnC·3Ca^{2+}·cTnI$_{34-71}$·cTnI$_{128-163}$ complex, only G70 shifts (Figure 3D). These results suggest that the W7 binding sites of W7 in the C-domain are blocked by cTnI$_{34-71}$, cTnI$_{128-147}$, or both, but W7 is capable of binding to the N-domain together with the switch region, cTnI$_{147-163}$. The chemical shift changes of G34, G42, G49, T53, E66, G68, G70, D73, and V79 are averaged and normalized according to the relation $(\delta_{obs} - \delta_{initial})/(\delta_{complex} - \delta_{initial})$. The normalized average data as a function of $[cTnC{\cdot}3Ca^{2+}{\cdot}cTnI_{34-71}{\cdot}cTnI_{128-163}]_{total}/[W7]_{total}$ ratio were fit to the following equation (see ref *7* and references therein):

$$cTnC{\cdot}3Ca^{2+}{\cdot}cTnI_{34-71}{\cdot}cTnI_{128-163} + W7 \rightleftarrows cTnC{\cdot}3Ca^{2+}{\cdot}cTnI_{34-71}{\cdot}cTnI_{128-163}{\cdot}W7$$

and yielded a macroscopic dissociation constant (K_D) of 0.5

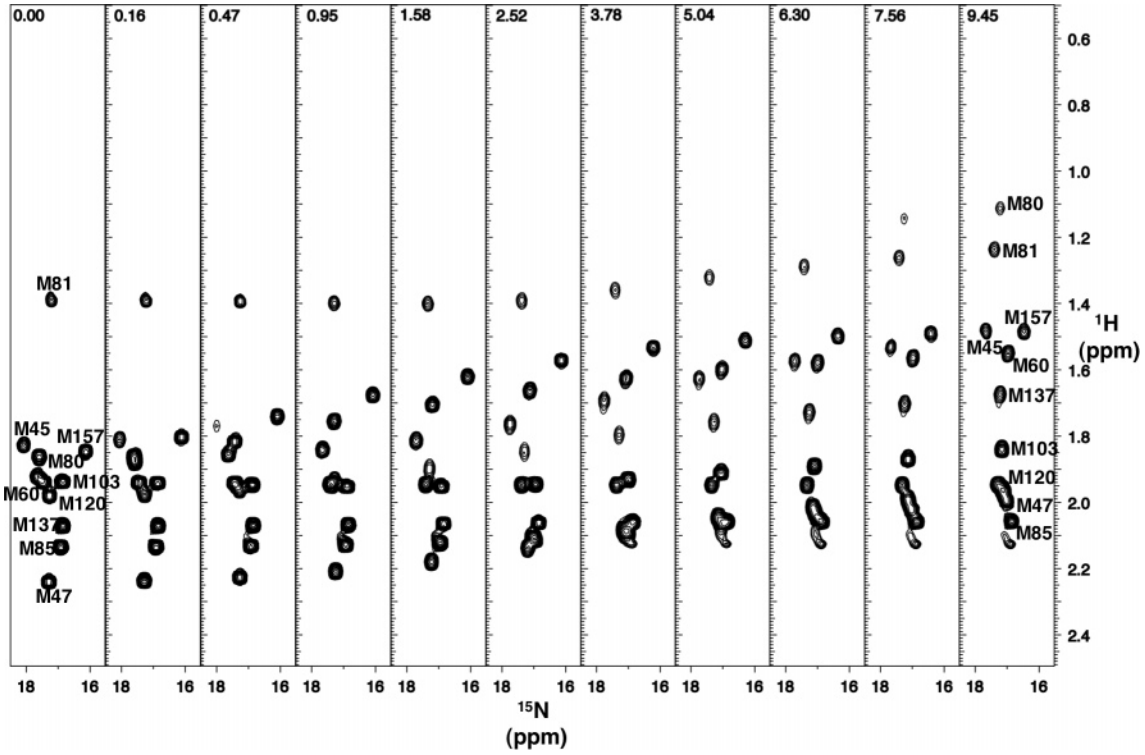

FIGURE 2: Titration of cTnC·3Ca^{2+} with W7. 2D ^{1}H−^{13}C HSQC NMR spectra from the methionine methyl regions of cTnC with various equivalents (shown at the top of each panel) of added W7.

± 0.1 mM (Figure 4). This affinity is very similar to that of Anapoe for the skeletal troponin complex ($K_D \sim 0.64$ mM) (*9*). It is likely that W7 binds in a fashion similar to that of Anapoe binding to sTnC and bepridil binding to cTnC (*18*).

DISCUSSION

The goal of this study is to assess if CaM antagonist W7 interacts with cTnC and how its binding to cTnC modulates the cTnC−cTnI interaction. To achieve this goal, we have utilized 2D ^{1}H−^{15}N and 2D ^{1}H−^{13}C HSQC NMR spectroscopy to monitor the binding of W7 to cTnC·3Ca^{2+} in the absence and presence of cTnI peptides. When cTnC·3Ca^{2+} is titrated with W7, the NMR peaks of backbone amides of almost all residues shift (Figure 1), suggesting the backbone of the entire protein has been perturbed. Analysis of the binding stoichiometry and the trajectories of chemical shift changes indicate that W7 binding occurs at multiple sites located in the N-domain, the C-domain, and the central linker of cTnC. Moreover, all the Met methyl groups located in the hydrophobic pocket of the two domains of cTnC exhibited high-field shifts (Figure 2), possibly due to ring current effects caused by the proximity of the W7 aromatic ring. These groups are from both the N-domain (e.g., M80 and M81) and the C-domain (e.g., M137 and M157) of cTnC. Similar high-field shifts have been reported in binding of W7 to isolated domains of cTnC (*25*) and binding of W7 (*30*), J-8 (a derivative of W7) (*26*), and TFP (*31*) to CaM·4Ca^{2+}. X-ray structure analysis revealed that CaM·4Ca^{2+}·TFP complexes (CaM·4Ca^{2+}:TFP ratio of 1:1 and 1:4) (*27*, *28*) adopt a globular structure similar to that of CaM·4Ca^{2+}−target peptide complexes (*32*). By using small-angle X-ray scattering as well as NMR spectroscopy, Osawa et al. (*24*) showed that binding of two molecules of W7 induces large structural changes in CaM·4Ca^{2+}; the overall shape changes from an elongated structure to a compact globular structure in solution, caused by bending of the flexible central linker. This phenomenon also occurs in the structure of the cTnC·3Ca^{2+}·3bepridil complex (*17*), which displays a globular shape resembling that of CaM·4Ca^{2+}·TFP and CaM·4Ca^{2+}−peptide complexes. On the basis of these comparisons, it is reasonable to suggest that a multisite mechanism for binding of W7 to cTnC may cause major structural changes in cTnC·3Ca^{2+}. One possibility is that cTnC·3Ca^{2+} undergoes a W7-induced interdomain compaction. As a result, the cTnC·3Ca^{2+}·W7 complex may adopt a globular shape resembling that of the cTnC·3Ca^{2+}·3bepridil complex (*17*). Thus, cTnC's known conformational plasticity, with respect to interdomain orientation, may be sensitive to W7 binding.

In the presence of cTnI$_{34-71}$ and cTnI$_{128-163}$ peptides, the binding of W7 to cTnC becomes much simpler and W7 binds specifically to the regulatory domain. The peptides used in this study contain the three important functional regions of cTnI that directly interact with cTnC; as such, the 1:1:1 complex (cTnC·3Ca^{2+}·cTnI$_{34-71}$·cTnI$_{128-163}$) presents a relevant model for W7 binding. A similar approach has been used to study the interaction of levosimendan with cTnC (*20*). Using isolated cTnC, at least three binding sites for levosimendan were identified (*33*); however, by using a cTnC·3Ca^{2+}·cTnI$_{32-79}$·cTnI$_{128-180}$ complex, it was shown that cTnI$_{32-79}$ blocks the levosimendan binding sites on the C-domain, whereas cTnI$_{128-180}$ does not compete with levosimendan for the binding site on the N-domain. This study allowed Sorsa et al. to conclude that the Ca^{2+}-sensitizing effect of levosimendan is located solely in the regulatory N-domain of cTnC (*20*). Our results show that in the 1:1:1 cTnC·3Ca^{2+}·cTnI$_{34-71}$·cTnI$_{128-163}$ complex, the

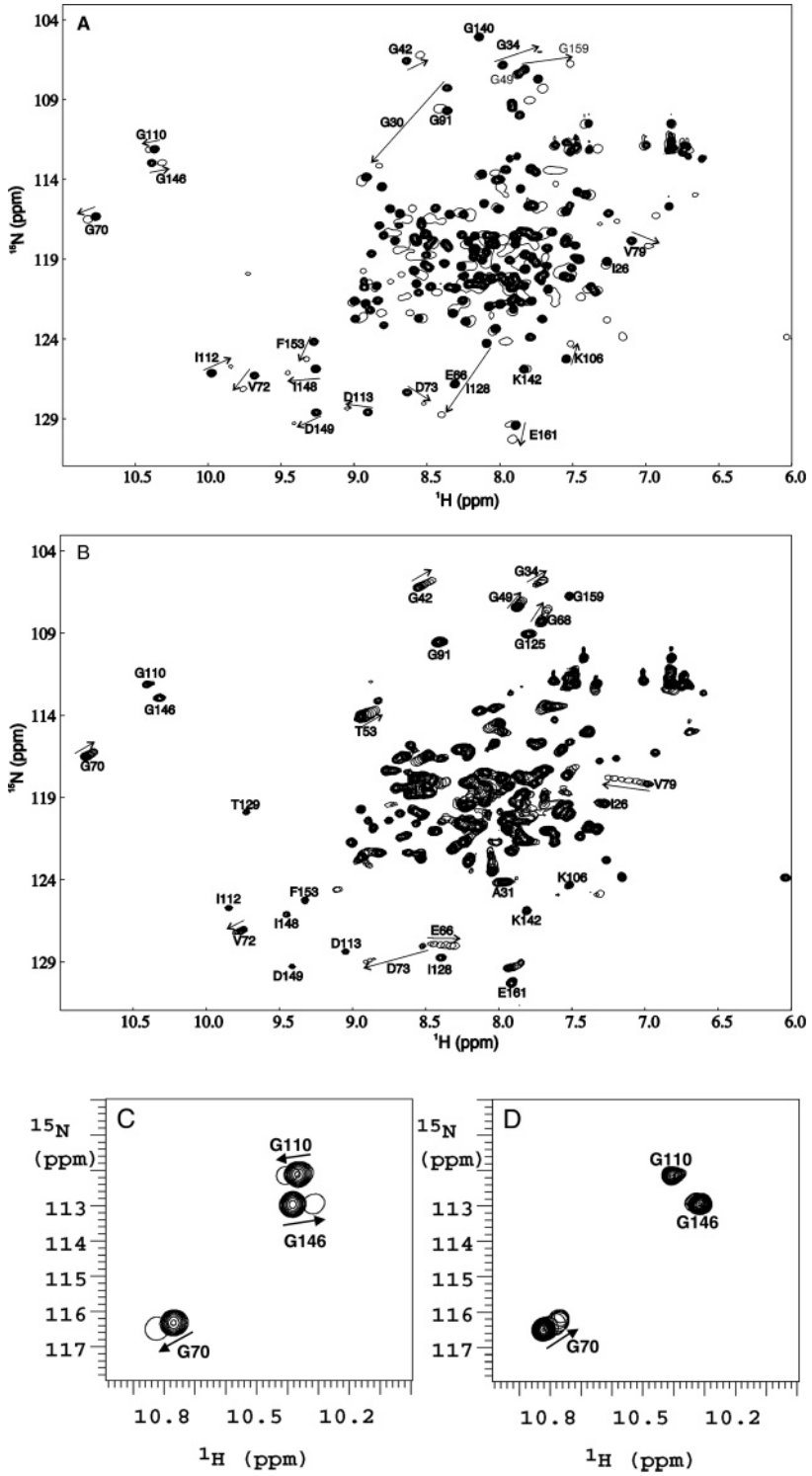

FIGURE 3: Titration of cTnC·3Ca^{2+} with cTnI$_{34-71}$ and cTnI$_{128-163}$ (A) and of the cTnC·3Ca^{2+}·cTnI$_{34-71}$·cTnI$_{128-163}$ complex with W7 (B). (A) The 2D ^{1}H−^{15}N HSQC NMR cross-peaks corresponding to cTnC·3Ca^{2+} are shown as multiple contours, whereas the peaks corresponding to the cTnC·3Ca^{2+}·cTnI$_{34-71}$·cTnI$_{128-163}$ complex are shown as single contours. (B) The 2D ^{1}H−^{15}N HSQC NMR cross-peaks corresponding to the cTnC·3Ca^{2+}·cTnI$_{34-71}$·cTnI$_{128-163}$ complex are shown as multiple contours, whereas the peaks at various W7 additions are shown as single contours. A selected region of panel A is shown in panel C and a selected region of panel B in panel D to demonstrate the chemical shift changes of the three signature glycine residues, G70 from Ca^{2+}-binding site I and G110 and G146 from Ca^{2+}-binding sites III and IV, respectively.

cTnI peptides block the binding sites for W7 in the C-domain of cTnC and that W7 binds to the regulatory domain of cTnC. Most importantly, this binding can occur in the presence of the switch region of cTnI.

We have shown previously that bepridil and the switch region of cTnI bind to cNTnC·Ca^{2+} concurrently (*18*). In the cNTnC·Ca^{2+}·cTnI$_{147-163}$·bepridil ternary complex, a binding site for cTnI$_{147-163}$ is primarily located on the AB interhelical interface and a binding site for bepridil is in the center of the hydrophobic pocket. A similar binding scenario is observed in the X-ray structure of the sTnC·4Ca^{2+}·sTnI$_{1-182}$·sTnT$_{156-262}$ complex (*9*); a detergent molecule,

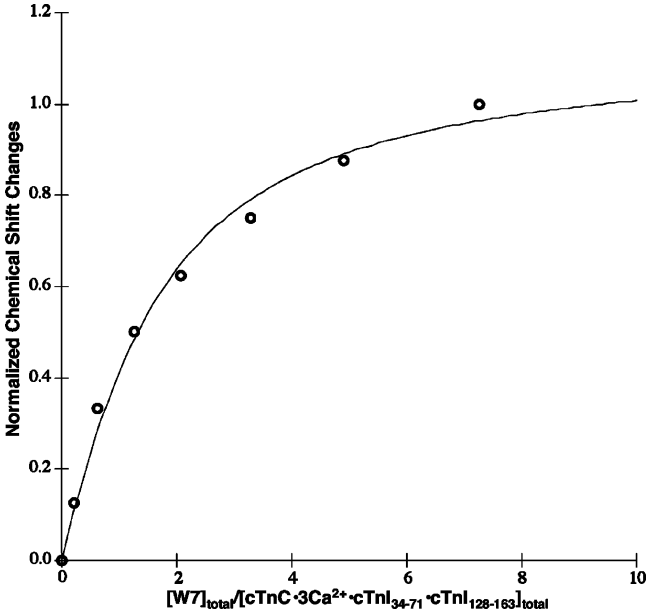

FIGURE 4: Titration of the cTnC·3Ca^{2+}·cTnI$_{34-71}$·cTnI$_{128-163}$ complex with W7. The chemical shift changes of G34, G42, G49, T53, E66, G68, G70, D73, and V79 are averaged and normalized according to the relation $(\delta_{obs} - \delta_{initial})/(\delta_{complex} - \delta_{initial})$. The best-fit curve to the data is shown as a solid line.

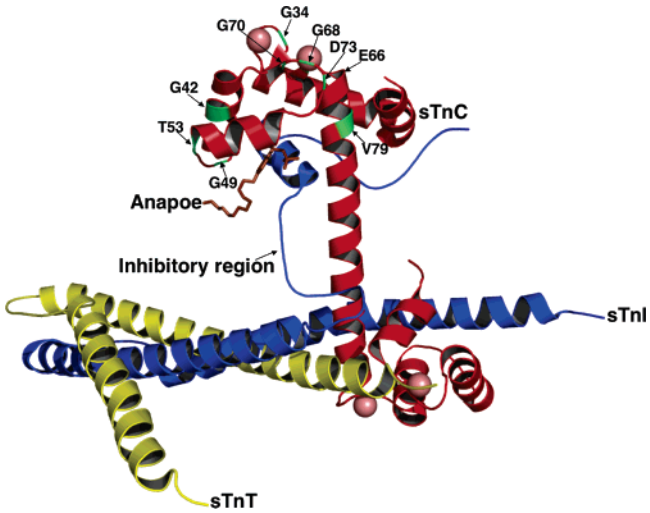

FIGURE 5: Ribbon representations of the X-ray structure of the sTnC·4Ca^{2+}·sTnI$_{1-182}$·sTnT$_{156-262}$·Anapoe complex (PDB entry 1YTZ). The protein subunits are color-coded as follows: red for sTnC, blue for sTnI, and yellow for sTnT. Pink spheres represent Ca^{2+} atoms. The residues corresponding to the cTnC residues (G34, G42, G49, T53, E66, G68, G70, D73, and V79) are colored green. The figure was created with PyMOL.

Anapoe, was found to bind together with the switch region of sTnI to the Ca^{2+}-saturated N-domain of sTnC (Figure 5), and this binding is responsible for the increase in the contractile force of muscle fibers in the presence of Anapoe (*9*). W7 appears to bind to a similar region where bepridil binds to the cNTnC·Ca^{2+}·cTnI$_{147-163}$ complex, and Anapoe binds to the sTnC·4Ca^{2+}·sTnI$_{1-182}$·sTnT$_{156-262}$ complex (Figure 5). This is supported by mapping the residues (G34, G42, G49, T53, E66, G68, G70, D73, and V79) that undergo W7-induced chemical shift changes (Figure 3B) on the X-ray structure of the sTnC·4Ca^{2+}·sTnI$_{1-182}$·sTnT$_{156-262}$ complex (Figure 5). These residues are conserved from human cTnC to chicken sTnC on the basis of primary sequence alignment, and they cluster around the binding site of Anapoe (Figure 5). This result demonstrates that the biologically relevant binding site of W7 is in the N-domain of cTnC and suggests that W7 may play a role in directly modulating the Ca^{2+} sensitivity of the regulatory domain of cTnC and the interaction of the switch region of cTnI and cTnC in cardiac myocytes.

The affinity determined for binding of W7 to the cTnC·3Ca^{2+}·cTnI$_{34-71}$·cTnI$_{128-163}$ complex ($K_D = 0.5 \pm 0.1$ mM) is comparable to that for binding of Anapoe to the sTnC·4Ca^{2+}·sTnI$_{1-182}$·sTnT$_{156-262}$ complex ($K_D \sim 0.64$ mM) and binding of levosimendan to the cTnC·3Ca^{2+}·cTnI$_{32-79}$·cTnI$_{128-180}$ complex ($K_D \geq 0.2$ mM) (*20*). This supports the notion that binding of W7 to cardiac troponin occurs in a mode similar to that of binding of levosimendan to cardiac troponin and binding of Anapoe to skeletal troponin. Note that these K_D values are in the millimolar range, which is generally considered weak for protein−drug interactions. It is possible that micellization of drug molecules in aqueous solutions contributes to this phenomenon (*34*, *35*). The dissociation constant for binding of W7 to the cTnC·3Ca^{2+}·cTnI$_{34-71}$·cTnI$_{128-163}$ complex is approximately 2 times greater than that reported for binding of W7 to the isolated N-domain of cTnC ($K_D = 0.22$ mM) (*25*). This difference suggests that the interaction between W7 and cTnC is weakened when the hydrophobic surface in the N-domain of cTnC is shared by W7 and the switch region of cTnI.

In the context of designing cardiotonic drugs, the current results add support to the growing body of evidence that most potential drug candidates (or their analogues) exert their effects in the regulatory N-domain of cTnC, by acting as either Ca^{2+} sensitizers (e.g., levosimendan and Anapoe) or Ca^{2+} desensitizers (e.g., W7). The net effect depends on which exact binding site is involved and whether this binding stabilizes or destabilizes the opening of the hydrophobic pocket and the interaction of cTnC with cTnI. A study by Kleerekoper et al. suggested that there are two drug binding sites in the N-domain hydrophobic pocket, with one site (marked by M45, M60, and M80) conferring Ca^{2+} sensitizing effects and the other site (containing M47, M81, and M85) also being capable of coordinating ligand but being capable of inhibiting the association of cTnC with cTnI or cTnI peptides and therefore conferring Ca^{2+} desensitizing effects (*16*). In the case of Anapoe, the detergent molecule interacts specifically with the hydrophobic side chains of eight amino acid residues of the N-domain of sTnC and also three hydrophobic residues of the switch region of sTnI. The net result is the stabilization of the hydrophobic pocket, corresponding to the facilitation of the binding of Ca^{2+} to the regulatory sites and enhancement of the contractile force of muscle fibers (*9*). Although the idea of Ca^{2+} sensitizers has been widely accepted, the idea of designing Ca^{2+} desensitizers may be useful considering the phenomenon of Ca^{2+} oversensitization in a majority of cardiomyopathies (*4*). W7 has been shown to act as a potent and reversible inhibitor of contraction in skeletal and heart muscle (*2*). Our results show that while binding of W7 to cardiac troponin may occur in a mode similar to that of binding of Anapoe to skeletal troponin, it may target the desensitizing site involving M47, M81, and M85 and may interfere with the binding of the switch region of cTnI to cTnC. Ca^{2+} desensitizers such as

W7 may be utilized in aiding muscle relaxation that is compromised under certain cardiac conditions.

The data presented in this work provide evidence to support the notion that cTnC is the primary target for the CaM antogonist W7 in the myofilament and the effective binding site of W7 is located in the regulatory domain of cTnC. The position of W7 in the cardiac troponin complex is analogous to that of Anapoe in the skeletal troponin complex. This is based on the observation that the binding of the switch region of TnI to the N-domain of TnC is the same in the X-ray structure of the cardiac troponin core complex, the solution NMR structure of the cNTnC·Ca^{2+}·$cTnI_{147-163}$ complex, and the X-ray structure of the skeletal troponin core complex. While it is not relevant to any conclusion drawn herein, we have discussed our data under the assumption that cardiac troponin behaves in solution in a manner consistent with recent models of the thin filament (*36*) derived from the skeletal troponin crystal structure (*9*); i.e., the central helix of cTnC is stabilized by the inhibitory region of cTnI (Figure 5). This is supported by the demonstration that the electrostatic force between the central helix of cTnC and the inhibitory region of cTnI is observed in the NMR solution structure of the cCTnC·$2Ca^{2+}$·$cTnI_{128-147}$ complex (*10*, *11*).

ACKNOWLEDGMENT

We thank David Corson and Melissa Rakovszky for expression and purification of the cTnC proteins used in this work and Jeff Devries for NMR spectrometer maintenance.

REFERENCES

1. Hidaka, H., Yamaki, T., Naka, M., Tanaka, T., Hayashi, H., and Kobayashi, R. (1980) Calcium-regulated modulator protein interacting agents inhibit smooth muscle calcium-stimulated protein kinase and ATPase, *Mol. Pharmacol. 17*, 66−72.
2. Adhikari, B. B., and Wang, K. (2004) Interplay of troponin- and myosin-based pathways of calcium activation in skeletal and cardiac muscle: The use of W7 as an inhibitor of thin filament activation, *Biophys. J. 86*, 359−370.
3. Sia, S. K., Li, M. X., Spyracopoulos, L., Gagné, S. M., Liu, W., Putkey, J. A., and Sykes, B. D. (1997) NMR structure of cardiac troponin C reveals an unexpected closed regulatory domain, *J. Biol. Chem. 272*, 18216−18221.
4. Li, M. X., Wang, X., and Sykes, B. D. (2004) Structural based insights into the role of troponin in cardiac muscle pathophysiology, *J. Muscle Res. Cell Motil. 25*, 559−579.
5. Spyracopoulos, L., Li, M. X., Sia, S. K., Gagné, S. M., Chandra, M., Solaro, R. J., and Sykes, B. D. (1997) Calcium-induced structural transition in the regulatory domain of human cardiac troponin C, *Biochemistry 36*, 12138−12146.
6. McKay, R. T., Saltibus, L. F., Li, M. X., and Sykes, B. D. (2000) Energetics of the induced structural change in a Ca^{2+} regulatory protein: Ca^{2+} and troponin I peptide binding to the E41A mutant of the N-domain of skeletal troponin C, *Biochemistry 39*, 12731−12738.
7. Li, M. X., Spyracopoulos, L., and Sykes, B. D. (1999) Binding of cardiac troponin-I 147−163 induces a structural opening in human cardiac troponin-C, *Biochemistry 38*, 8289−8298.
8. Takeda, S., Yamashida, A., Maeda, K., and Maeda, Y. (2003) Structure of the core domain of human cardiac troponin in the Ca^{2+}-saturated form, *Nature 424*, 35−41.
9. Vinogradova, M. V., Stone, D. B., Malanina, G. G., Karatzaferi, C., Cooke, R., Mendelson, R. A., and Fletterick, R. J. (2005) Ca^{2+}-regulated structural changes in troponin, *Proc. Natl. Acad. Sci. U.S.A. 102*, 5038−5043.
10. Lindhout, D. A., and Sykes, B. D. (2003) Structure and dynamics of the C-domain of human cardiac troponin C in complex with the inhibitory region of human cardiac troponin I, *J. Biol. Chem. 278*, 27024−27034.
11. Lindhout, D. A., Boyko, R. F., Corson, D. C., Li, M. X., and Sykes, B. D. (2005) The role of electrostatics in the interaction of the inhibitory region of troponin I with troponin C, *Biochemistry 44*, 14750−14759.
12. Arteaga, G. M., Kobayashi, T., and Solaro, R. J. (2002) Molecular actions of drugs that sensitize cardiac myofilaments to Ca^{2+}, *Ann. Med. 34*, 248−258.
13. Rosevear, P. R., and Finley, N. (2003) Molecular mechanism of levosimendan action: An update, *J. Mol. Cell. Cardiol. 35*, 1011−1015.
14. Sorsa, T., Pollesello, P., and Solaro, R. J. (2004) The contractile apparatus as a target for drugs against heart failure: Interaction of levosimendan, a calcium sensitizer, with cardiac troponin C, *Mol. Cell. Biochem. 266*, 87−107.
15. Kass, D. A., and Solaro, R. J. (2006) Mechanisms and use of calcium-sensitizing agents in the failing heart, *Circulation 113*, 305−315.
16. Kleerekoper, Q., Liu, W., Choi, D., and Putkey, J. A. (1998) Identification of binding sites for bepridil and trifluoperazine on cardiac troponin C, *J. Biol. Chem. 273*, 8153−8160.
17. Li, Y., Love, M. L., Putkey, J. A., and Cohen, C. (2000) Bepridil opens the regulatory N-terminal lobe of cardiac troponin C, *Proc. Natl. Acad. Sci. U.S.A. 97*, 5140−5145.
18. Wang, X., Li, M. X., and Sykes, B. D. (2002) Structure of the regulatory N-domain of human cardiac troponin C in complex with human cardiac troponin $I_{147-163}$ and bepridil, *J. Biol. Chem. 277*, 31124−31133.
19. Wang, X., Li, M. X., Spyracopoulos, L., Beier, N., Chandra, M., Solaro, R. J., and Sykes, B. D. (2001) Structure of the C-domain of human cardiac troponin C in complex with the Ca^{2+} sensitizing drug EMD 57033, *J. Biol. Chem. 276*, 25456−25466.
20. Sorsa, T., Pollesello, P., Permi, P., Drakenberg, T., and Kilpelainen, I. (2003) Interaction of levosimendan with cardiac troponin C in the presence of cardiac troponin I peptides, *J. Mol. Cell. Cardiol. 35*, 1055−1061.
21. Li, M. X., Saude, E. J., Wang, X., Pearlstone, J. R., Smillie, L. B., and Sykes, B. D. (2002) Kinetic studies of calcium and cardiac troponin I peptide binding to human cardiac troponin C using NMR spectroscopy, *Eur. Biophys. J. 31*, 245−256.
22. Tripet, B. P., Van Eyk, J. E., and Hodges, R. S. (1997) Mapping of a second actin-tropomyosin and a second troponin C binding site within the C-terminus of troponin I, and their importance in the Ca^{2+} dependent regulation of muscle contraction, *J. Mol. Biol. 271*, 728−750.
23. Delaglio, F., Grzesiek, S., Vuister, G. W., Zhu, G., Pfeifer, J., and Bax, A. (1995) NMRPipe: A multidimensional spectral processing system based on UNIX pipes, *J. Biomol. NMR 6*, 277−293.
24. Osawa, M., Kuwamoto, S., Izumi, Y., Yap, K. L., Ikura, M., Shibanuma, T., Yokokura, H., Hidaka, H., and Matsushima, N. (1999) Evidence for calmodulin inter-domain compaction in solution induced by W-7 binding, *FEBS Lett. 442*, 173−177.
25. Hoffman, R. M. B., Li, M. X., and Sykes, B. D. (2005) The binding of W7, an inhibitor of striated muscle contraction, to cardiac troponin C, *Biochemistry 44*, 15750−15759.
26. Craven, C. J., Whitehead, B., Jones, S. K., Thulin, E., Blackburn, G. M., and Waltho, J. P. (1996) Complexes formed between calmodulin and the antagonists J-8 and TFP in solution, *Biochemistry 35*, 10287−10299.
27. Cook, W. J., Walter, L. J., and Walter, M. R. (1994) Drug binding by calmodulin: Crystal structure of a calmodulin-trifluoperazine complex, *Biochemistry 33*, 15259−15265.
28. Vandonselaar, M., Hickie, R. A., Quail, J. W., and Delbaere, L. T. (1994) Trifluoperazine-induced conformational change in Ca^{2+}-calmodulin, *Nat. Struct. Biol. 1*, 795−801.
29. Kleerekoper, Q., and Putkey, J. A. (1999) Drug binding to cardiac troponin C, *J. Biol. Chem. 274*, 23932−23939.
30. Osawa, M., Swindells, M. B., Tanikawa, J., Tanaka, T., Mase, T., Furuya, T., and Ikura, M. (1998) Solution structure of calmodulin-W-7 complex: The basis of diversity in molecular recognition, *J. Mol. Biol. 276*, 165−176.
31. Klevit, R. E., Levine, B. A., and Williams, R. J. P. (1981) A study of calmodulin and its interaction with TFP by high resolution ^1H NMR spectroscopy, *FEBS Lett. 123*, 25−29.
32. Ikura, M., Clore, G. M., Gronenborn, A. M., Zhu, G., Klee, C. B., and Bax, A. (1992) Solution structure of a calmodulin-target

peptide complex by multidimensional NMR, *Science 256*, 632−638.
33. Sorsa, T., Heikkinen, S., Abbott, M. B., Abusamhadneh, E., Laakso, T., Tilgmann, C., Serimaa, R., Annila, A., Rosevear, P. R., Drakenberg, T., Pollesello, P., and Kilpelainen, I. (2001) Binding of levosimendan, a calcium sensitizer, to cardiac troponin C, *J. Biol. Chem. 276*, 9337−9343.
34. Attwood, D., and Natarajan, R. (1981) Effect of pH on the micellar properties of amphiphilic drugs in aqueous solution, *J. Pharm. Pharmacol. 33*, 136−140.
35. Ravin, L. J., and Warren, R. J. (1971) Micelle formation and its significance in interpretation of NMR spectra of phenothiazine, *J. Pharm. Sci. 60*, 329.
36. Pirani, A., Vinogradova, M. V., Curmi, P. M., King, W. A., Fletterick, R. J., Craig, R., Tobacman, L. S., Xu, C., Hatch, V., and Lehman, W. (2006) An atomic model of the thin filament in the relaxed and Ca^{2+}-activated states, *J. Mol. Biol. 357*, 707−717.

BI060779A